

Submitted to ISMRM 2023, Toronto, Canada

An open-source, low-cost 8-channel transmit/receive 3T head coil for pTx developments, MR safety testing and standardization

Christoph Stefan Aigner¹, Mads Sloth Vinding², Lukas Winter¹, Reiner Montag¹, Sebastian Schmitter^{1,3,4}, Bernd Ittermann¹, Frank Seifert¹

¹*Physikalisch-Technische Bundesanstalt (PTB), Braunschweig and Berlin, Germany*

²*Center of Functionally Integrative Neuroscience (CFIN), Department of Clinical Medicine, Faculty of Health, Aarhus University, Aarhus, Denmark*

³*Medical Physics in Radiology, German Cancer Research Center (DKFZ), Heidelberg, Germany*

⁴*Center for Magnetic Resonance Research, University of Minnesota, Minneapolis, MN, United States*

Summary of main findings

An open-source, low-cost head coil with eight TX/RX channels is presented for reproducible pTx method development and/or safety assessments. Phantom measurements validate the predicted B_1^+ fields and demonstrate the capabilities of this RF coil.

Synopsis

This work investigates an open-source, low-cost, 8-channel transmit/receive head coil to enable rapid and reproducible pTx development, safety assessment and evaluation at 3T. FDTD simulations were validated with phantom measurements on a 3T with an external pTx system. Relative and absolute 2D/3D B_1^+ -maps were acquired to compute the CP+ mode, and two RF shims were tailored to enforce B_1^+ efficiency and homogeneity. The open-access design files could serve as a basis for new RF coil designs or pTx projects without needing high expertise in RF coil development or as a cost-effective alternative for multi-centre studies.

Abstract

Introduction:

MRI is driven to increased magnetic fields for higher signal-, contrast-to-noise ratio and spectral resolution. Parallel transmission (pTx) is beneficial to improve flip angle (FA) homogeneity, reduce local and global SAR, or enable mitigation of RF-induced implant heating.^{1,2} However, researchers typically need access to a 7T system with a commercial pTx system for pTx method developments and/or safety studies. Since not every research group has access to a 7T, more and more home-built (broadband) pTx electronics have been developed in the community that can be hooked to a single-channel scanner. Unfortunately, most commercially available pTx RF coils only target 7T and are high-cost, closed-source, and inflexible due to a fixed or complex coil design that is difficult to replicate without high expertise in RF-coil development. Moreover, a cost-effective and easy-to-build pTx RF coil solution has the potential to become the new standard for multi-centre or comparative studies because it is much cheaper to build a second coil than to order a commercial one or send a coil back and forth. Here we research and build our own 8-channel TX/RX head coil (<5000€) for 3T applications and make all design files publicly available to enable researchers to replicate the pTx coil quickly. Experimentally acquired 2D/3D relative/absolute B_1^+ maps and GRE data with tailored RF shims validate the electromagnetic field simulations and B_1^+ predictions.

Methods:

The proposed 3T pTx RF coil design is based on an existing 7T pTx loop RF coil³. The design translation, 7T→3T, resulted in two significant modifications of eased manufacturing complexity. First, the RF shield could be omitted due to much lower radiation losses at 3T and, secondly, loop element lengths were increased from 160mm to 250mm to enable whole brain imaging and match the lower Larmor frequency. The in-house manufactured loop elements were mounted on a non-conductive frame in an elliptical fashion (7T loop element angles preserved), and plastic rods and a 3D-printed phantom holder for a cylindrical grid phantom⁴ were added to improve the mechanical stability of the coil. Each loop element carries five capacitors, one trimmable for fine-tuning, optimized through simulations⁵. To maintain symmetry, the capacitance at the loop's feeding port was split in half by two equal capacitors. For typical loading conditions, the impedance at the feeding ports is between 10Ω-15Ω. Thus, we realized an impedance matching via a 1:4 transformation in the balun, which was needed because of the required symmetrical drive of the coil element. The balun consists of a half-wave line and two quarter-wave lines. The latter was realized by two 50Ω coaxial cables connected in parallel to achieve the 1:4 transformation. The use of high voltage-resistant components (>1kV) allows for at least 1kW of RF power per channel. MRI was performed on a pTx capable 3T scanner (Siemens Verio, Germany) using an external 8x8kW amplifier (Analogic AN8135S8) and a home-built TX/RX switch box³. Absolute 2D and 3D B_1^+ -maps were acquired and reconstructed with a magnitude-based preparation pulse method⁶ and the AFI approach⁷, respectively. Relative 2D/3D B_1^+ -maps were also obtained.⁸ Phase only RF shimming was performed for a region of interest.⁹ 2D/3D GRE scans with parameters fitting to the B_1^+ -scans were acquired to validate the pTx approaches. The RF coil design files are available at <https://gitlab1.ptb.de/mri-lab/8ch-ptx-headcoil-3t>.

Results and Discussion:

Fig.1 shows the schematic of the proposed coil scaffold, its FDTD voxel grid, and the assembled 8-channel TX/RX RF coil with all eight loop elements.

Fig.2A shows the circuit schematics of three of the eight elements and the optimized capacitor values to tune and decouple the loops using the variable capacitors (Fig.2B). The measured S matrix (Fig.2C) reflects the simulated parameters and results in a coil coupling of nearest neighbor elements of approximately 8 dB with much less coupling to the other elements. The power loss due to the couplings is around 30%, excluding internal power losses.

Fig.3 shows one representative RF channel's simulated and measured absolute B_1^+ -maps (2D preparation-based method). As expected, there is a good agreement between simulated and measured absolute B_1^+ -maps with a scaling factor of 1.45, consistent with the measured voltage losses due to cable loss and TX/RX switch. A similar trend was observed for all eight RF channels (not shown), with an average of $7\mu\text{T}/\sqrt{\text{kW}}$ and a range of $4,93\mu\text{T}/\sqrt{\text{kW}}$ and $9,82\mu\text{T}/\sqrt{\text{kW}}$. The combined (all channels) B_1^+ efficiency (CP+ mode; not shown) of the coil in the center is about $35\mu\text{T}/\sqrt{\text{kW}}$.

Fig.4 shows 2D channel-wise relative B_1^+ -maps together with a 3D GRE scan using the CP+ superposition and 3D AFI maps in a phantom. For the CP+ mode, the signal maximum occurs in the phantom's center, but if desired, e.g., for single-voxel spectroscopy, it can be steered to other areas of interest with little loss in intensity by different RF shims.

Fig.5 shows the results of three different RF shim settings: (i) random, (ii) effective, and (iii) homogeneous RF shim. Qualitatively, there is a good match between the B_1^+ prediction, RF efficiency and the acquired 2D GRE scan.

Conclusion:

This work describes the development of a low-cost, easy-to-build, open-source, 8TX/8RX 3T head coil that allows rapid pTx development, safety assessment and 3T pTx applications. In addition, the open-access design files could serve as a basis for new RF coil design or pTx research without needing high expertise in RF coil development.

References:

- 1) Padormo, F., Beqiri, A., Hajnal, J. V., and Malik, S. J. (2016), Parallel transmission for ultrahigh-field imaging. *NMR Biomed.*, 29: 1145– 1161. doi: <https://doi.org/10.1002/nbm.3313>
- 2) Winter L, Seifert F, Zilberti L, Murbach M, Ittermann B. MRI-Related Heating of Implants and Devices: A Review. *Journal of Magnetic Resonance Imaging* 53:1646–1665 doi: <https://doi.org/10.1002/jmri.27194>
- 3) Seifert, F, Pfeiffer, H, Mekle, R, Waxmann, P and Ittermann, B. 7T 8-channel pTx head coil with high B_1^+ efficiency optimized for MRS. Proc. 24th Annu. Meet. ISMRM, Singapore, Singapore: Abstract 3545; 2016.
- 4) Brühl, R, Ihlenfeld A, Aydin, S, et al. On the comparability of volumetric brain data in the multicentric IMAGEN study. Proc. 21st Annu. Meet. ISMRM, Salt Lake City, Utah, USA: Abstract 893; 2013.
- 5) Seifert, F, Wübbeler, G, Junge, S, Ittermann, B and Rinneberg, H. Patient safety concept for multichannel transmit coils. *J Magn Reson Imaging*, 26(5):1315–21, 2007. doi: <https://doi.org/10.1002/jmri.21149>
- 6) Yarnykh, V.L. (2007), Actual flip-angle imaging in the pulsed steady state: A method for rapid three-dimensional mapping of the transmitted radiofrequency field. *Magn Reson Med*, 57: 192-200. doi: <https://doi.org/10.1002/mrm.21120>
- 7) Van de Moortele P, Ugurbil K. Very fast multi channel B_1 calibration at high field in the small flip angle regime. Proc. 17th Annu. Meet. ISMRM, Honolulu, Hawaii, USA: Abstract 367; 2009.
- 8) Dietrich, S, Aigner, CS, Kolbitsch, C, et al. 3D Free-breathing multichannel absolute B_1^+ Mapping in the human body at 7T. *Magn Reson Med*. 2021; 85: 2552– 2567. doi: <https://doi.org/10.1002/mrm.28602>
- 9) Aigner, CS, Dietrich, S, Schmitter, S. Three-dimensional static and dynamic parallel transmission of the human heart at 7 T. *NMR Biomed*. 2021; 34:e4450. doi: <https://doi.org/10.1002/nbm.4450>

Acknowledgements:

This work has received funding from the German Research Foundation (SCHM 2677/4-1, GRK2260), VILLUM FONDEN and the European Partnership on Metrology, co-financed by the European Union's Horizon Europe Research and Innovation Programme and by the Participating States, under grant number 21NRM05 STASIS.

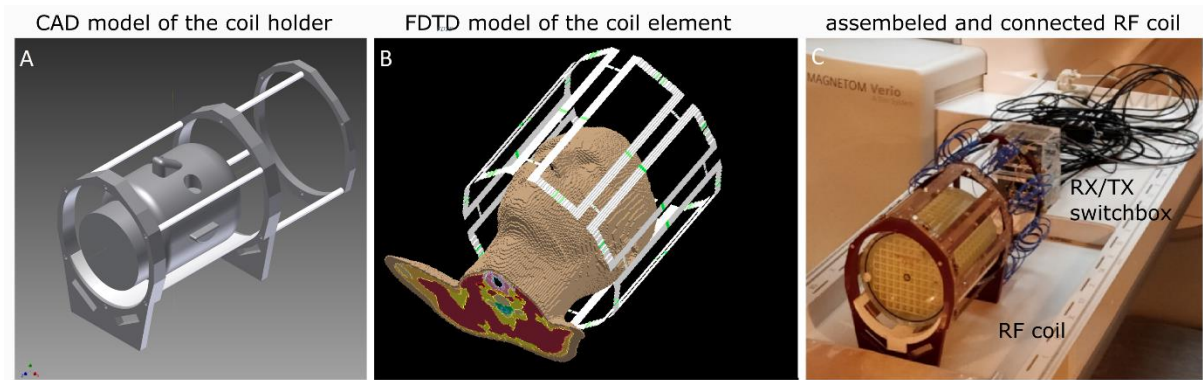


Figure 1: (A): The computer-aided design (CAD) model of the proposed coil; (B): Finite-difference time-domain (FDTD) model of the eight coil elements and Duke's body model; (C): Assembled RF coil including baluns and the connection to the RX/TX switch box and the used 3T system.

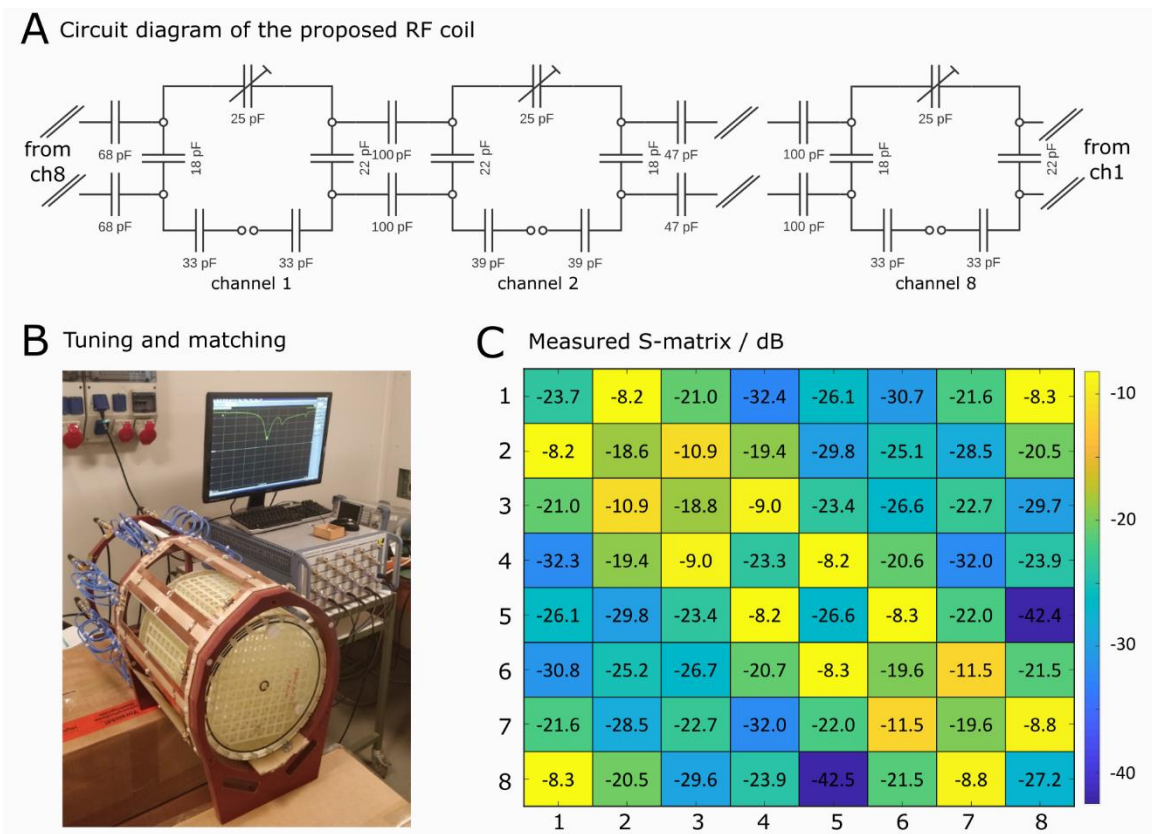


Figure 2: Circuit schematics (three out of eight loops are shown) of the proposed pTx coil (A), Tuning and matching with the trimmable conductor and using a network analyzer (B), and measured S-matrix of the proposed coil loaded with a uniform cylindrical phantom that simulates the head's coil loading.

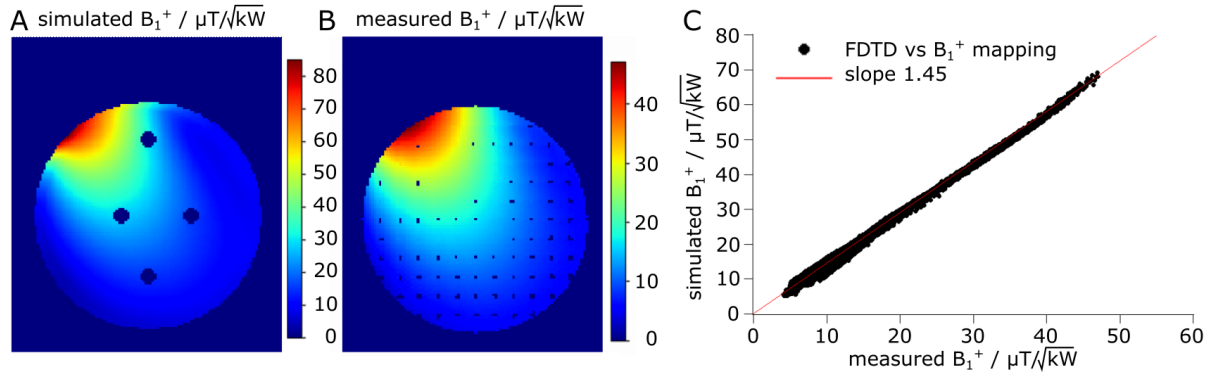


Figure 3: Validation of the simulated B_1^+ of channel 1 (A) and measured B_1^+ of channel 1 in a matching phantom (B); elements 2-8 were left open. The quantitative comparison of simulated and measured B_1^+ shows a scaling factor of 1.45 (the pixel-wise evaluation has been performed in the masked phantom region, see Fig.3A and B), consistent with the measured voltage losses due to cable loss and TX/RX switch. The other channels resulted in a similar trend (not shown).

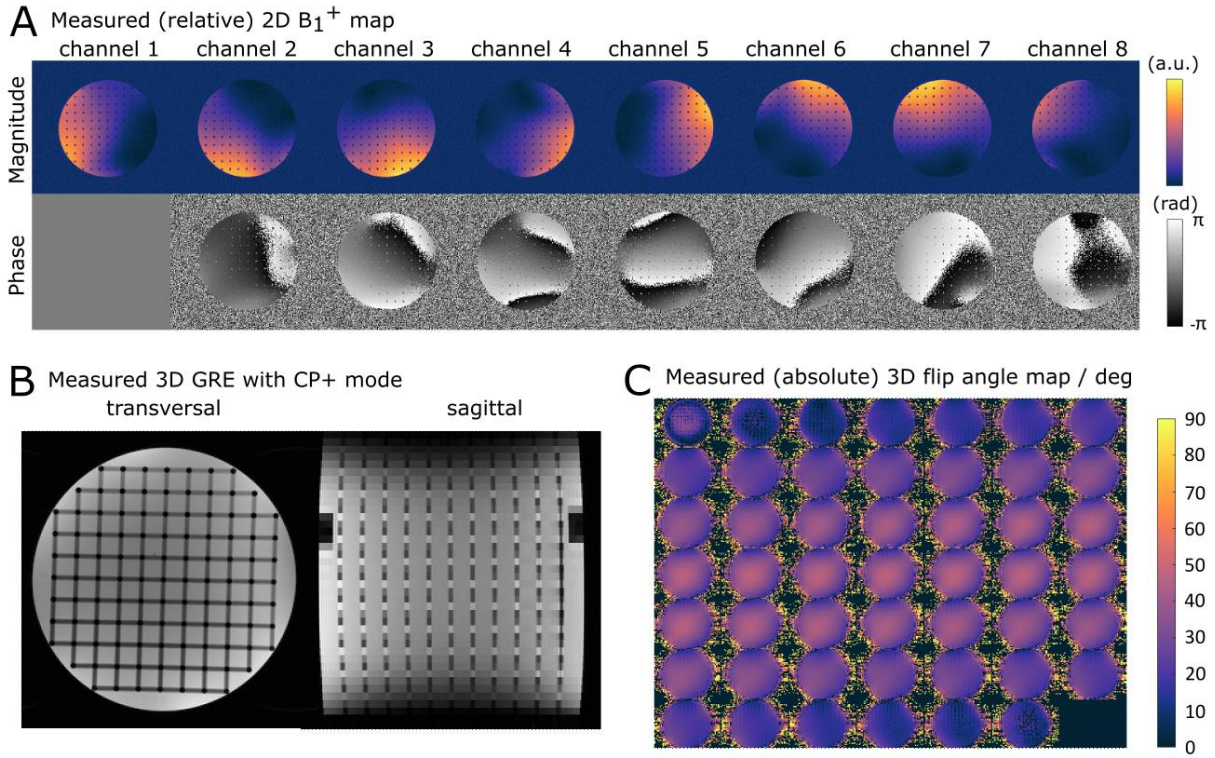


Figure 4: 2D relative B_1^+ maps (magnitude and phase) are shown (A) to compute the CP+ mode (constructive phase interference). The CP+ mode is used to acquire a 3D GRE volume (B) and to measure 3D flip angle maps (C). For the CP+ mode, the signal maximum occurs in the phantom's centre, but using the pTx capabilities of the scanner, it can be steered to other areas of interest with little loss in intensity.

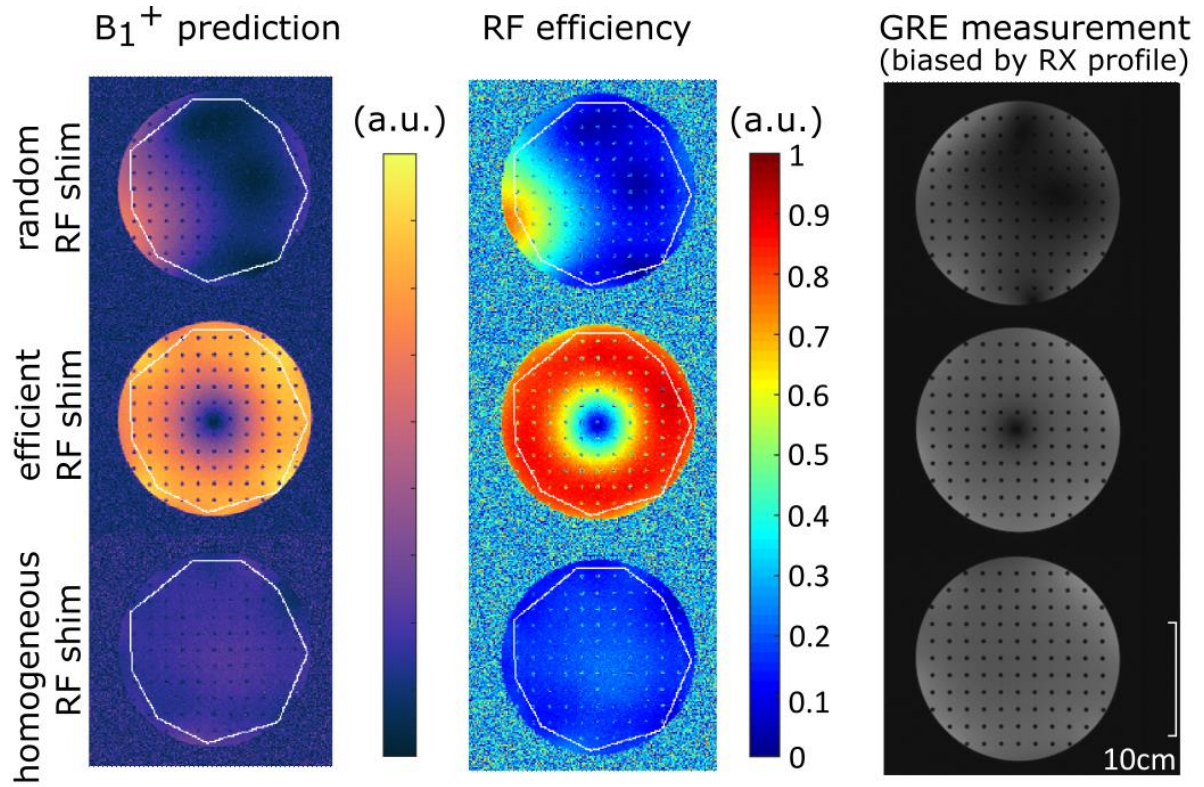


Figure 5: B_1^+ -predictions, RF efficiency and GRE measurements for three different RF shims. The RF shims are computed based on measured relative B_1^+ -maps (see Figure 4). The white outline is the region of interest. The efficient RF shim reduces the coefficient of variation (CV) from 76% (random RF shim) to 29.4% and improves the mean efficiency from 20.6% (random RF shim) to 73.3%. The homogeneous shim achieves a CV of 20.5% and a mean efficiency of 16.6% to reach a homogeneous flip angle across the region of interest.